


Article

Coupling Coordination Relationship between Urban Sprawl and Urbanization Quality in the West Taiwan Strait Urban Agglomeration, China: Observation and Analysis from DMSP/OLS Nighttime Light Imagery and Panel Data

Chunyan Lu ^{1,*} , Lin Li ² , Yifan Lei ¹, Chunying Ren ³, Ying Su ¹, Yufei Huang ¹, Yu Chen ⁴ , Shaohua Lei ⁵  and Weiwei Fu ¹

¹ College of Computer and Information Sciences, Fujian Agriculture and Forestry University, Fuzhou 350002, China; leiylf@fafu.edu.cn (Y.L.); suying@fafu.edu.cn (Y.S.); huangyf@fafu.edu.cn (Y.H.); fuweiwei@fafu.edu.cn (W.F.)

² Department of Earth Sciences, Indiana University-Purdue University Indianapolis, Indianapolis, IN 46202, USA; ll3@iupui.edu

³ Key Laboratory of Wetland Ecology and Environment, Northeast Institute of Geography and Agroecology, Chinese Academy of Sciences, Changchun 130102, China; renchy@iga.ac.cn

⁴ Key Laboratory of Digital Earth Science, Aerospace Information Research Institute, Chinese Academy of Sciences, Beijing 100094, China; chenyu@radi.ac.cn

⁵ School of Geography, Nanjing Normal University, Nanjing 210023, China; 171301035@stu.njnu.edu.cn

* Correspondence: luchunyan@fafu.edu.cn; Tel.: +86-137-6380-5686

Received: 28 August 2020; Accepted: 30 September 2020; Published: 2 October 2020



Abstract: Urban sprawl is the most prominent characteristic of urbanization, and increasingly affects local and regional sustainable development. The observation and analysis of urban sprawl dynamics and their relationship with urbanization quality are essential for framing integrative urban planning. In this study, the urban areas of the West Taiwan Strait Urban Agglomeration (WTSUA) were extracted using nighttime light imagery from 1992 to 2013. The spatio-temporal characteristics and pattern of urban sprawl were quantitatively analyzed by combining an urban expansion rate index and a standard deviation ellipse model. The urbanization quality was assessed using an entropy weight model, and its relationship with urban sprawl was calculated by a coupling coordination degree model. The results showed that the urban area in the WTSUA experienced a significant increase, i.e., 18,806.73 km², during the period 1992–2013. The central cities grew by 11.08% and noncentral cities by 27.43%, with a general uneven city rank-size distribution. The urban sprawl showed a circular expansion pattern, accompanied by a gradual centroid migration of urban areas from the southeast coast to the central-western regions. The coupling coordination level between urban expansion and urbanization quality increased from serious incoordination in 1992 to basic coordination in 2013. Dual driving forces involving state-led policies and market-oriented land reform had a positive influence on the harmonious development of urban sprawl and urbanization quality of the WTSUA. This research offers an effective approach to monitor changes in urban sprawl and explore the coupling coordination relationship between urban sprawl and urbanization quality. The study provides important scientific references for the formulation of future policies and planning for sustainable development in urban agglomerations.

Keywords: urban sprawl; urbanization quality assessment; nighttime light imagery; coupling coordination degree; rank-size rule; West Taiwan Strait Urban Agglomeration

1. Introduction

Urban sprawl is a prevalent phenomenon worldwide because of accelerating population growth and global urbanization [1–3]. Its manifestation through the evolution of regional urban systems has far-reaching impacts on urban economic, social, and eco-environmental development. The harmonization of urban sprawl with eco-environment and socio-economic interests is crucial to the sustainable development of urban systems [4]. In recent decades, the urbanization process has been gradually transformed from the traditional urbanization mode to the new-type urbanization path, with a focus on the “quality” of urbanization, which has a greater emphasis of eco-environment conservation and human well-being improvement [5]. Furthermore, when urban centers expand and become clustered around large cities [6], urban agglomerations form and dominate regional urban economic and social development [7,8]. Then, the relationship between urban sprawl and urbanization quality becomes more complicated [9]. Under such circumstances, studies on the coordination relationship between urban sprawl and urbanization quality are a top priority because they help to develop knowledge-based urban planning strategies and actualize effective urban sprawl paths, which are vital for social stability, economic prosperity, and ecological safety [10,11].

Urban sprawl in the world has followed different paths. In most western countries, market-oriented land use contributes to urban sprawl, showing a leapfrog (i.e., noncontiguous, or scattered), low density, and single-use urban development pattern [12,13]. In contrast, urban sprawl in China is characterized by high-density housing projects, multifunctional community construction, and rapid expansion, driven by the coexistence of state-led, top-down planning policy and market-regulated, bottom-up demand [10,14]. Many empirical studies on urban sprawl have been carried out to determine its trends, intensity, driving forces, evolution, and future scenarios [5,15,16]. However, in contrast to the rich literature on developed regions and countries, urban sprawl in emerging urban agglomerations has not been fully investigated. As such, it is essential for urban agglomerations to analyze the range and intensity of urban sprawl systematically, as well as to identify the main influencing factors to facilitate effective strategic decision making.

An enormous number of studies on urbanization quality have been conducted by qualitative and quantitative methods [17–19]. For example, Zhou et al. [9] developed a conceptual comprehensive index system of urbanization quality assessment from the perspective of the structure and function of an urban system. Lin et al. [20] proposed a comprehensive assessment system of urbanization quality including demographic urbanization, spatial urbanization, economic urbanization, and social urbanization to analyze the effects of urbanization on the eco-environment. Wang et al. [18] and Martínez-Zarzoso [21] evaluated urbanization quality and examined the relationship between it and CO₂ emissions in China and several developing countries, respectively. However, existing research has seldom focused on the interaction mechanisms between urbanization quality and urban sprawl.

Remote sensing (RS) and geographic information systems (GIS) are common tools for analyzing urban sprawl at different spatial scales [22,23]. Remote sensing allows the change and distribution of urban areas to be delineated more effectively [24], while GIS enables valuable spatial information to be analyzed [25]. For example, QuickBird and Worldview-2 images were used to detect the changing trend and spatial characteristics of urban sprawl in one Indian city [24]. Landsat TM/ETM+ images were used to detect and analyze urban change in a rapidly urbanizing region of China and in Pune metropolis, India [23,26]. The spatio-temporal evolution of urban agglomerations of bay areas in the US, China and Japan were detected and compared using Landsat TM/OLI [27]. Because of the low classification efficiency of traditional optical image data, time-discontinuous images are often used to extract urban areas, leading to the omission of detailed changes over long periods [28]. In contrast, nighttime light images well represent the spatial extent of urban areas and have advantages in studying urban dynamics on large spatial scales or with high temporal frequencies [29–32]. For example, Castells-Quintana [33] and Li et al. [34] used nighttime light images to analyze the urban pattern and economic growth in sub-Saharan Africa and in the countries along “The Belt and Road”, respectively. Huang et al. [35] detected changes in the city size dynamics in China from 1992 to 2008 and discovered that urban

areas extracted from nighttime light imagery were more accurate than census data. Stokes and Seto divided cities into different categories using nighttime light data to explore whether infrastructure was synchronized with land and demographic transitions [36]. Generally, nighttime light images are valuable for characterizing urban expansion at regional, national, and global scales [28,37], and it is worth exploring the potential of this data type in the study of urban sprawl dynamics. However, few studies have systematically explored urbanization quality based on nighttime light radiance variation, which has seriously impeded the application of nighttime light data in urban development [38].

The West Taiwan Strait Urban Agglomeration (WTSUA) is situated on the southeast coast, across the Taiwan Strait from Taiwan Province, China, and plays a vital role in strengthening the communication and cooperation between Mainland China and Taiwan Province [39]. Given the advantages of nighttime light imagery in reflecting urban dynamics, as well as the importance of revealing the interaction between urban sprawl and urbanization quality, the objectives of this research were to: (1) extract and map urban areas of the WTSUA; (2) characterize the dynamics of urban sprawl in terms of intensity, rank-size, and expansion pattern; (3) assess the urbanization quality; and (4) determine the coupling relationship between urban sprawl and urbanization quality over time. This analysis will provide valuable information for urban policymakers and planners to formulate urban development strategies. To fulfill these objectives, time-series nighttime light images were used to extract urban areas. The urban expansion rate index (UERI), standard deviation ellipse (SDE), and rank-size rule (RSR) model were used to calculate the urban sprawl intensity, sprawl pattern, and city-size distribution dynamics, respectively. The entropy weight (EW) model was used to evaluate the urbanization quality of the WTSUA. A coupling coordination degree (CCD) model was applied to quantify the relationship between urban sprawl and the urbanization quality of urban agglomeration.

2. Materials and Methods

2.1. Study Area

The WTSUA is located to the west of Taiwan Strait, China. The longitude ranges from 22.82° N to 29.57° N and the latitude ranges from 113.86° E to 121.23° E, with a total area of 2.70×10^5 km² and a total population of about 9.42×10^7 in 2018. It consists of four provinces, Fujian, Zhejiang, Jiangxi, and Guangdong, including 20 prefecture-level administrative cities (Table 1 and Figure 1). The five central cities are in the eastern coastal region, and the fifteen noncentral cities are mostly situated in the central-western region. The average annual precipitation is 1249–2985 mm, and the annual mean temperature is 15–23 °C. The prevalent climate of this region is a subtropical monsoon climate, characterized by a hot and rainy summer and a warm and wet winter. More than 75% of the region is covered by natural forests, which provides suitable habitat for numerous wildlife species, and it possesses more ecological resources than other urban agglomerations in China.

In December 2009, the “Coordinated Development Planning for West Taiwan Strait Urban Agglomeration”, a major national program for promoting the development of the WTSUA, was officially issued, marking the start of a more detailed and concrete development strategy and target for the WTSUA. By virtue of its convenient transport networks, geographical location, and support from the state, the WTSUA has become one of China’s most important economic zones. Furthermore, the region is becoming a platform for exchange and cooperation with global influence. The GDP of the WTSUA reached 5.87 trillion Yuan in 2018, accounting for 6.52% of China’s GDP.

Table 1. Basic information description of each city in WTSUA.

Province	City	Area (10 ⁴ km ²)	Population (Million Person) *	GDP (10 ² Billion-Yuan) *	Code
Fujian	Fuzhou	1.19	7.74	7.86	FZ
Fujian	Xiamen	0.18	4.11	4.79	XM
Fujian	Putian	0.40	2.90	2.24	PT
Fujian	Sanming	2.25	2.58	2.35	SM
Fujian	Quanzhou	1.11	8.70	8.47	QZ
Fujian	Zhangzhou	1.30	5.14	3.95	ZZ
Fujian	Nanping	2.59	2.69	1.79	NP
Fujian	Longyan	1.88	2.64	2.39	LY
Fujian	Ningde	1.29	2.91	1.94	ND
Jiangxi	Yingtian	0.36	1.28	0.82	YT
Jiangxi	Shangrao	2.30	6.81	2.21	SR
Jiangxi	Ganzhou	3.94	9.81	2.81	GZ
Jiangxi	Fuzhou	1.86	4.05	1.38	FZa
Zhejiang	Wenzhou	1.14	9.25	6.01	WZ
Zhejiang	Quzhou	0.88	2.21	1.47	QZa
Zhejiang	Lishui	1.67	2.70	1.39	LS
Guangdong	Shantou	0.22	5.64	2.51	ST
Guangdong	Chaozhou	0.32	2.66	1.07	CZ
Guangdong	Meizhou	1.56	4.38	1.11	MZ
Guangdong	Jieyang	0.54	6.09	2.15	JY

* represents the information documented in 2018.

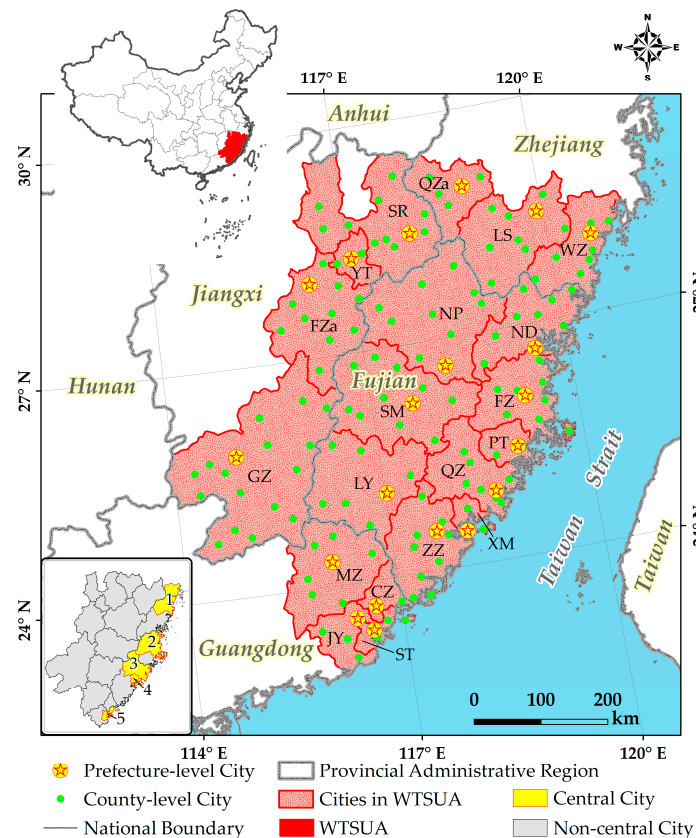


Figure 1. Location of the study area (WTSUA represents the West Taiwan Strait Urban Agglomeration; QZa: Quzhou city, LS: Lishui city, WZ: Wenzhou city, ND: Ningde city, NP: Nanping city, FZ: Fuzhou city in Fujian province, SM: Sanming city, PT: Putian city, QZ: Quanzhou city, XM: Xiamen city, ZZ: Zhangzhou city, LY: Longyan city, CZ: Chaozhou city, ST: Shantou city, JY: Jieyang city, MZ: Meizhou city, SR: Shangrao city, YT: Yingtian city, FZa: Fuzhou city in Jiangxi province, GZ: Ganzhou city; 1, 2, 3, 4, and 5 represent Wenzhou city, Fuzhou city in Fujian province, Quanzhou city, Xiamen city, and Shantou city, respectively).

2.2. Nighttime Light Imagery and Pre-Processing

To analyze the urban sprawl dynamics of the WTSUA, a time series dataset from the DMSP/OLS (Defense Meteorological Satellite Program's Operational Linescan System) was used with a spatial resolution is 1 km. The DMSP/OLS dataset provides yearly nighttime light images for the period of 1992–2013, and records nighttime light through a DN (digital number) value for each pixel, i.e., from 0 to 63. A value of '0' represents no light in the area, and a value of '63' indicates maximum brightness.

Compared with other publicly available nighttime light imagery, i.e., NPP-VIIRS (National Polar-orbiting Partnership Visible Infrared Imaging Radiometer Suite), Luojia 1-01, and Jilin 1-03b, the DMSP/OLS data eliminate the effects of fires, lighting, moonlight, clouds and auroras, reducing the error caused by background noise. Furthermore, each DMSP/OLS image is acquired from 8:30 to 9:30 pm locally, while the NPP-VIIRS satellite passes over at about 01:30 am. Nighttime lights captured earlier, especially at around 9:00 pm, are likely to include light sources from residents, roads, commercial areas, and industrial sites. When nighttime lights are measured around midnight, some of these light sources may no longer contribute, depending on lifestyles in different regions [40]. On the other hand, although Luojia 1-01 (spatial resolution is 130 m) [41] and Jilin 1-03b (spatial resolution is 0.89 m) [42] nighttime light data are superior in spatial resolution, radiometric detection range, and onboard calibration, their available time spans are 2018 to the present and 2017 to the present, respectively; as such, it would be difficult to undertake long-term research using them [38,43,44]. Therefore, DMSP/OLS data are more representative and suitable for long-term analyses of urban areas than other nighttime light data.

The DMSP/OLS time series data were acquired from six different DMSP satellites, i.e., F10 (1992–1994), F12 (1994–1999), F14 (1997–2003), F15 (2000–2007), F16 (2004–2009), and F18 (2010–2013). Datasets acquired by different satellites in the same year or by the same satellite over different years are not comparable until they are radiometrically calibrated. As referenced by Hu et al. [40], the DMSP/OLS data were calibrated from 1992 to 2013. After systematic calibration, the urban areas of the WTSUA from 1992 to 2013 were extracted using the thresholding technique [28]. Due to considerable regional variation in socio-economic development status and physical environment, it was difficult to select a single threshold to distinguish the urban areas. Therefore, the WTSUA was divided into two regions, i.e., coastal region and inland region. The former includes WZ, ND, FZ, PT, QZ, XM, ZZ, CZ, JY, and ST. The latter includes LS, NP, SM, LY, MZ, QZa, SR, YT, FZa, and GZ. The threshold was determined automatically by the method of maximum interclass variance, also known as the OTSU algorithm [45]. First, 10,000 random points in 1995, 2000, 2005, and 2010 were generated in the urban areas according to the auxiliary data which were the land cover data for 1995, 2000, 2005, and 2010, provided by the National Earth System Science Data Center, China. Then, the DN value of each point was extracted in the corresponding years. Next, the optimal thresholds for 1995, 2000, 2005, and 2010 were calculated by the OTSU method for each region. Finally, the determined thresholds were applied to different stages, i.e., the thresholds for 1995, 2000, 2005, and 2010 were applied to the periods 1992–1997, 1998–2002, 2003–2008, and 2009–2013, respectively.

After the urban areas of each year had been extracted, the accuracy verification dataset of the extracted urban areas was produced. Specifically, 100 urban patches were chosen randomly from the 2010 land cover data. Then, the urban patches in 1995, 2000, and 2005 were also extracted based on land cover data for 1995, 2000, and 2005, which corresponded spatially to the 100 patches in 2010. Finally, the urban areas of the remaining years located in the 100 random patches were mapped by visual interpretation using Landsat TM/OLI images. All of these constituted the accuracy validation dataset, which was used to evaluate the accuracy of extracted urban areas by the DMSP/OLS data. As referenced by Ma et al. [46], a polygon-based validation method was used to validate the extraction accuracy of urban areas by DMSP/OLS data, showing that the overall accuracy for each year was higher than 0.89, and the average overall accuracy is 0.91 ± 0.02 .

2.3. Measurement of Urban Sprawl Dynamics

2.3.1. Urban Expansion Rate Index

To describe the speed of urban expansion objectively in spatial terms, an UERI was calculated, which may be expressed as follows [47]:

$$UERI = \frac{U_b - U_a}{U_a} \times \frac{1}{T} \times 100\% \quad (1)$$

where U_a is the urban area at the beginning year of the study periods, U_b is the end year of the study periods, and T is the number of years. Time intervals considered in this research were 1992–1999, 1999–2006, and 2006–2013.

2.3.2. Standard Deviation Ellipse

The morphological characteristics of the distribution of urban areas, e.g., range, direction, and centroid, make it possible to provide a more intuitive description of the trends of urban sprawl to determine the pattern and process of urban change. To achieve this, the SDE model was chosen to calculate the centrality, orientation, and shape of the urban distribution [48]. The area of the ellipse represents the region in which urban areas are spatially dominant. The azimuth of the ellipse reflects the principal tendency of urban distribution. The centroid is the center of all urban areas in two-dimensional space. Changes in the urban centroid over time can reflect the overall evolutionary route of urban sprawl. The minor and major axes of the ellipse indicate the directions and scope of the urban distribution and the dispersion degree among different urban regions [49]. A greater difference between the minor and major axes indicates a more obvious polarization phenomenon. The elements of SDE are expressed as follows [50]:

$$X_w = \frac{\sum_{i=1}^n w_i x_i}{\sum_{i=1}^n w_i}, Y_w = \frac{\sum_{i=1}^n w_i y_i}{\sum_{i=1}^n w_i} \quad (2)$$

$$\tan \theta = \frac{(\sum_{i=1}^n x_i^2 - \sum_{i=1}^n y_i^2) + \sqrt{(\sum_{i=1}^n x_i^2 - \sum_{i=1}^n y_i^2)^2 + 4 \sum_{i=1}^n x_i^2 y_i^2}}{2 \sum_{i=1}^n x_i^2 y_i^2} \quad (3)$$

$$SDE_x = \sqrt{\frac{\sum_{i=1}^n (x_i - x_i)^2}{n}} \quad (4)$$

$$SDE_y = \sqrt{\frac{\sum_{i=1}^n (y_i - y_i)^2}{n}} \quad (5)$$

where (x_i, y_i) are the geographic coordinates of the i th urban area, w_i is a weight, (x_w, y_w) are the weighted means of the i th urban area. (X_w, Y_w) is the centroid of the ellipse. SDE_x is the length of the long axis of the ellipse, and SDE_y is the short axis of the ellipse. θ represents the ellipse directional orientation, indicating the clockwise rotation degree from north to the ellipse long axis.

2.3.3. Rank-Size Rule Model

A comparison of the evenness of change in city size over time is vital to measure the intercity concentration in the urban agglomeration system [35]. To quantify the distribution dynamics of city

size for the WTSUA, the RSR model was applied to quantify the vertical dimension of the urban agglomeration system, which is calculated as follows [51]:

$$\lg P_i = \lg P_1 - q \lg R_i \quad (6)$$

where P_1 is the largest city's urban area in WTSUA, P_i is the urban area of the city which is ranked i th by urban area. R_i is the number of cities with city size bigger than P_i . q is the Pareto coefficient that denotes the distribution evenness of city size. When $q = 1$, the city size is directly proportional to the largest city size and the reciprocal of its rank. When $q < 1$, the distribution of city size is less even, indicating that there are only a small number of large-sized cities. In contrast, when $q > 1$, the distribution of city size is more even. The temporal change of q can reflect the relationship between the centralization force and dispersion force of city-size distribution. If the value of q presents an increasing tendency, the intercity centralization force is greater than its dispersion force, and vice versa.

2.4. Urbanization Quality Assessment

2.4.1. Establishment of an Assessment System for Urbanization Quality

Understanding urbanization quality is a complex and multidimensional task. To assess urbanization quality, a well-diversified evaluation system was developed [9,20]. Given the data availability and comparability over the study period, as well as their relevance to the assessment objective, panel data of twenty-eight basic variables were selected to assess urbanization quality from 1992 to 2013. These indicators are described in Table 2. The original values for all evaluation variables were derived from the China City Statistical Yearbook and the China Statistical Yearbook.

Table 2. Evaluation indicator system of urbanization quality.

Purpose	First-Grade Index	Basic Index
Urbanization Quality	Eco-environment Status	X_1 Per capita water resources (m^3/person)
		X_2 Per capita land area ($\text{hm}^2/\text{person}$)
		X_3 Per capita gas supply volume (m^3/person)
		X_4 Per capita green areas (m^2)
		X_5 Treatment rate of domestic sewage (%)
		X_6 Landfill rate for urban waste (%)
	Social Well-being Level	X_7 Proportion of built-up area to total area (%)
		X_8 Per capita urban road area in municipal district (m^2)
		X_9 Per capita public library holdings (volume)
		X_{10} Proportion of science and technology expenditure to GDP (%)
		X_{11} Proportion of educational expenditure to GDP (%)
		X_{12} Number of teachers per 1000 students (unit)
		X_{13} Per capita housing (m^2/person)
		X_{14} Number of medical beds per 1000 persons (unit)
		X_{15} Registered urban unemployment rate (%)
		X_{16} Number of buses per 1000 persons (unit)
	Econo-demographic Development	X_{17} Proportion of population in municipal district to total population (%)
		X_{18} Population density in municipal district ($\text{person}/\text{km}^2$)
		X_{19} Proportion of secondary and tertiary industry employment to total employment (%)
		X_{20} Per capita investment in fixed assets (Yuan/person)
		X_{21} Per capita GDP (Yuan/person)
		X_{22} Per capita GDP in the secondary and tertiary industry (Yuan/person)
		X_{23} GDP (100 million yuan)
		X_{24} Per capita disposable income of urban residents (Yuan)
		X_{25} Total retail sales of consumer goods (100 million yuan)
		X_{26} Proportion of secondary and tertiary industry GDP to total GDP (%)
		X_{27} Per capita local government fiscal revenue (Yuan)
		X_{28} Financial institution deposits at year-end (100 million Yuan)

2.4.2. Entropy Weight Model

The EW model is used to describe the relative importance of each indicator for the overall assessment objective. Several evaluation methods can be used for calculating weights, e.g., analytic hierarchy process [52], Delphi [53], principal component analysis [54], and artificial neural networks [55]. The EW model can determine an index's weight based on the value of information entropy for the index itself, which avoids the influence of subjective bias from different decision-makers [56,57]. Moreover, the approach is not only time-saving, but could also reduce the deviations caused by the discrepancies between different evaluated objects [58]. Therefore, it can reflect the relationship among indices objectively and efficiently. In this study, urbanization quality was evaluated by the EW model.

2.5. Coupling Coordination Degree Model

A CCD model was used to measure the coordination relationship between urban sprawl and urbanization quality. The CCDM can be expressed as follows [59]:

$$C = \frac{2\sqrt{f(x) \cdot g(y)}}{f(x) + g(y)} \quad (7)$$

$$T = \alpha f(x) + \beta g(y) \quad (8)$$

$$D = \sqrt{C \cdot T} \quad (9)$$

where $g(y)$ and $f(x)$ are the function of urban sprawl and urbanization quality, respectively. C is the coupling degree of urban sprawl and urbanization quality. T reflects the overall coordination level of the urban sprawl and urbanization quality. D is the CCD of urban sprawl and urbanization quality; the higher its value, the higher the coupling coordination level. Both α and β are the weights of urban sprawl and urbanization quality to be determined. Considering that urban sprawl plays a vital role in urbanization quality in the WTSUA, the weights are supposed to be equal, i.e., $\alpha = \beta = 0.5$ [60].

As referenced by Xing et al. [59] as well as Wen and Wen [61], the coupling coordination relationship between urban sprawl and urbanization quality can be described by dividing the CCD into different categories. In this study, the coupling coordination level was compartmentalized into six types, as shown in Table 3.

Table 3. Classification type of coupling coordination degree between urban sprawl and urbanization quality.

Coordination Level	Coupling Coordination Degree	Coupling State	Coordination Characteristics
Serious incoordination	[0.0, 0.4]	Low coupling phase	Serious disparity exists between urban expansion extent and urbanization quality level. The urban system development is degenerating.
Moderate incoordination	(0.4, 0.5]	Low coupling phase	Moderate disparity exists between urban expansion extent and urbanization quality level. It is basically acceptable in the short term.
Slight incoordination	(0.5, 0.6]	Antagonism phase	Slight disparity exists between urban expansion extent and urbanization quality level. It is acceptable in the short term.
Basic coordination	(0.6, 0.7]	Running-in phase	Urban expansion extent is basically synchronized with urbanization quality level.
Moderate coordination	(0.7, 0.8]	Running-in phase	Urban expansion extent is moderately synchronized with urbanization quality level, and it is ideal.
High coordination	(0.8, 1.0]	High coupling phase	Urban expansion extent is highly synchronized with urbanization quality level, and it is the most ideal.

3. Results

3.1. Spatio-Temporal Characteristics of Urban Sprawl

3.1.1. Dynamic Change of Total Nighttime Light Inventory

By calibrating the DMSP/OLS data for each year systemically, we could compare and analyze all the nighttime light images of the WTSUA during the period 1992–2013 under a unified standard. Figure 2 illustrates the spatio-temporal variations in nighttime light and the change in total nighttime light inventory of the WTSUA. The results indicated that the total nighttime light amount of the WTSUA increased during 1992–2013, with a change rate of 520.89%. Compared with the eastern coastal areas, there was a more dramatic increase for the nighttime lights in central-western inland areas. The increase rates of the central-western inland areas and the eastern coastal areas from 1992 to 2013 were 605.74% and 465.07%, respectively. The nighttime light proportion of the eastern coastal areas decreased from 60.25% in 1992 to 54.82% in 2013, while the nighttime light proportion of central-western inland areas increased from 39.75% in 1992 to 45.18% in 2013.

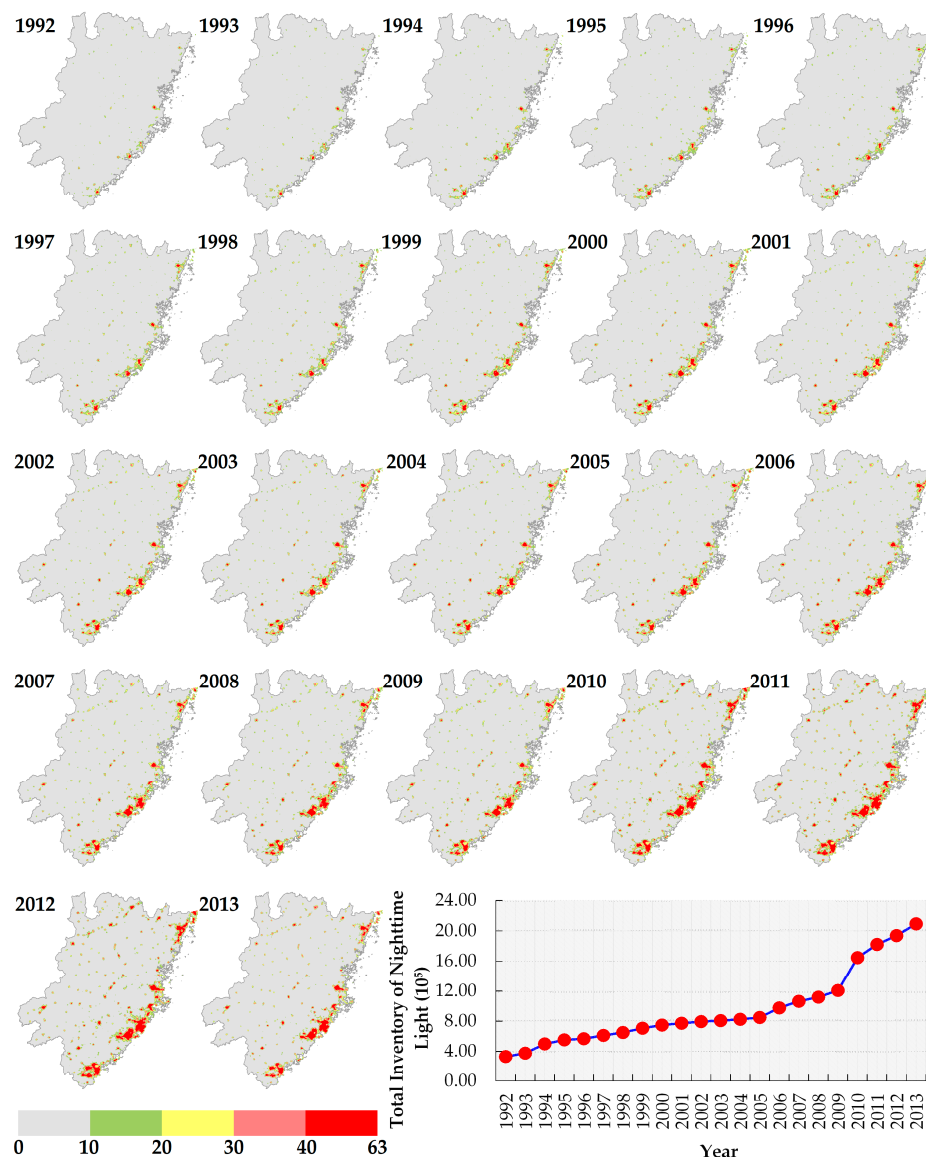


Figure 2. Spatio-temporal change of nighttime light from 1992 to 2013 in WTSUA.

3.1.2. Rate, Intensity, and Pattern of Urban Sprawl

After automatically extracting urban areas in each year based on the OTSU threshold method, the speed, intensity, and pattern of urban expansion were analyzed. Table 4 shows the expansion area and spatial expansion rate of urban areas for different city types. The results indicated that the urban areas of each city experienced a general increasing trend from 1992 to 2013, with a total growth rate of 895.56 km²/y for the WTSUA. During 1992–1999 and 1999–2006, the urban areas of central cities expanded more than those of noncentral cities. In contrast, the urban areas of noncentral cities exhibited a dramatic increase from 2006 to 2013, which was more than 1.5 times the total expansion area of central cities in this stage. In terms of the sprawl intensity, the spatial expansion rate of noncentral cities in urban areas was always higher than that of central cities from 1992 to 2013, indicating a higher value of UERI. Except for Xiamen city, the urban expansion areas of central cities all exceeded those of noncentral cities over the 22 years. Zhangzhou city showed the largest expansion in noncentral cities, increasing by 1517.16 km² from 1992 to 2013.

Figure 3 illustrates the spatio-temporal dynamics of SDE elements for urban sprawl from 1992 to 2013. Despite slight fluctuations, the SDE centroid showed a process of shifting northwest throughout the study period (Figure 3a), implying a stronger expansion power for cities located in the central-western regions of the WTSUA. The spatial distribution area of SDE for urban areas experienced a persistent increasing trend (Figure 3b), suggesting an increasing expansion of the main urban distribution areas. It is noteworthy that the SDE azimuth changed from 35.53° in 1992 to 44.67° in 2013, presenting a trend of gradually rotating southeast (Figure 3c). These results suggest that the urban sprawl force driven by the central-western inland cities (belonging to noncentral cities) exceeded that from the eastern coastal cities (mostly belonging to central cities) over time.

The spatio-temporal sprawl pattern of urban areas in the WTSUA is displayed in Figure 4. A cycloid expansion model of urban areas was found for each city from 1992 to 2013, showing that urban areas expanded gradually in circular or semicircular patterns, with their initial area as the center. The urban sprawl of the total urban agglomeration demonstrated a multi-nuclei pattern as a whole, including three main cores, i.e., the Wenzhou, Fuzhou–Quanzhou–Xiamen, and Shantou regions.

Table 4. Changes in area and expansion rate of urban areas for different city types in the WTSUA.

City Type	City Name	1992–1999				1999–2006				2006–2013			
		Total Change Area/km ²	Total UERI/%	Change Area/km ²	UERI/%	Total Change Area/km ²	Total UERI/%	Change Area/km ²	UERI/%	Total Change Area/km ²	Total UERI/%	Change Area/km ²	UERI/%
Central City	WZ	2661.07	46.46	616.77	132.24	2092.83	8.59	468.75	9.80	4313.86	11.06	966.44	11.98
	FZ			301.39	23.20			332.05	9.74			1388.02	24.21
	QZ			995.42	87.84			726.28	8.97			1183.12	8.97
	XM			286.47	24.86			353.35	11.19			288.91	5.13
	ST			461.02	27.49			212.40	4.33			487.38	7.63
Noncentral City	PT	1555.06	62.63	175.51	72.01	1661.61	12.42	139.15	9.45	6520.78	26.07	542.05	22.16
	SM			82.27	32.52			64.55	7.79			395.06	30.85
	ZZ			245.29	63.28			188.44	8.95			1083.43	31.64
	NP			61.77	48.04			38.11	6.79			387.64	46.83
	LY			93.85	69.11			103.05	13.00			374.41	24.73
	ND			70.92	331.95			21.31	4.11			355.10	53.24
	YT			32.47	204.69			45.31	18.64			147.34	26.30
	SR			33.91	58.41			124.08	42.00			470.08	40.39
	GZ			40.87	27.04			264.15	60.42			609.95	26.68
	FZa			15.14	142.86			76.56	65.67			357.50	54.79
	QZa			72.81	38.50			85.55	12.24			326.44	25.16
	LS			49.81	236.00			122.96	33.25			420.47	34.17
	CZ			188.54	50.74			205.76	12.17			206.32	6.59
	MZ			128.13	61.69			82.73	7.49			238.90	14.19
	JY			263.80	87.74			99.91	4.65			606.08	21.29
All cities		4216.13	51.35			3754.44	9.95			10,834.64	16.92		

Note: UERI denotes expansion rate index of urban areas; WZ: Wenzhou city, FZ: Fuzhou city in Fujian province, QZ: Quanzhou city, XM: Xiamen city, ST: Shantou city, PT: Putian city, SM: Sanming city, ZZ: Zhangzhou city, NP: Nanping city, LY: Longyan city, ND: Ningde city, YT: Yingtan city, SR: Shangrao city, GZ: Ganzhou city, FZa: Fuzhou city in Jiangxi province, QZa: Quzhou city, LS: Lishui city, CZ: Chaozhou city, MZ: Meizhou city, JY: Jieyang city.

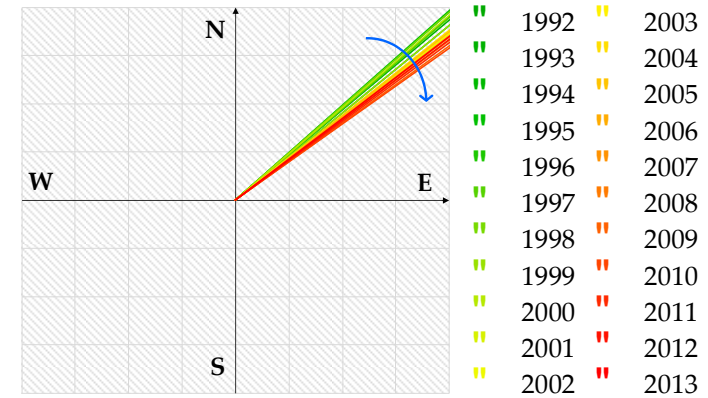
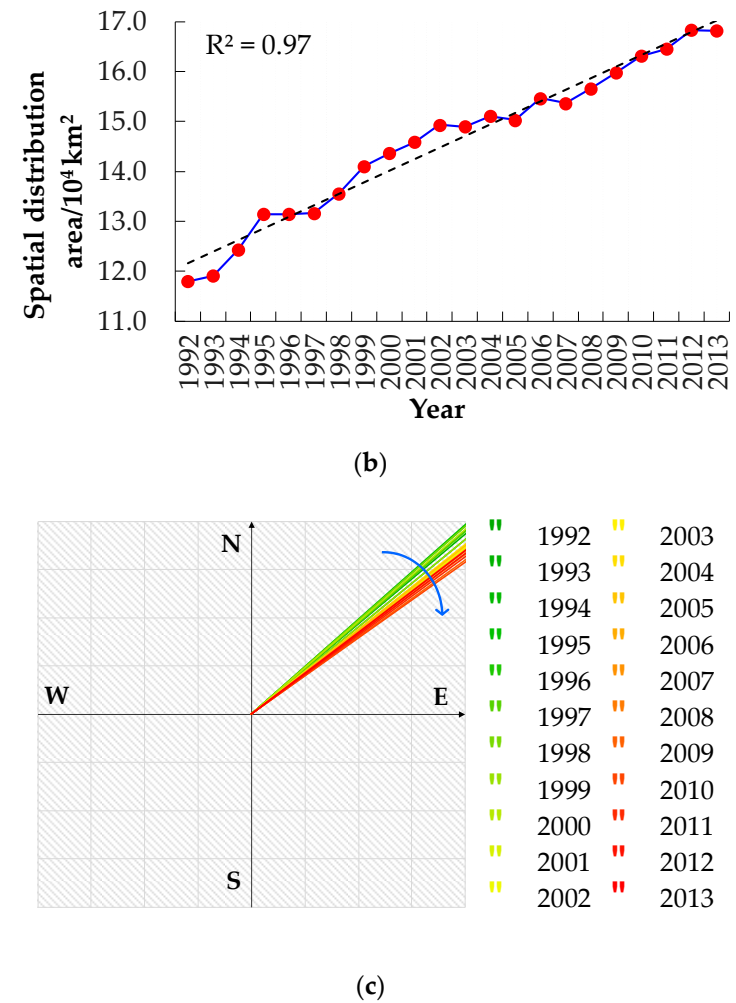
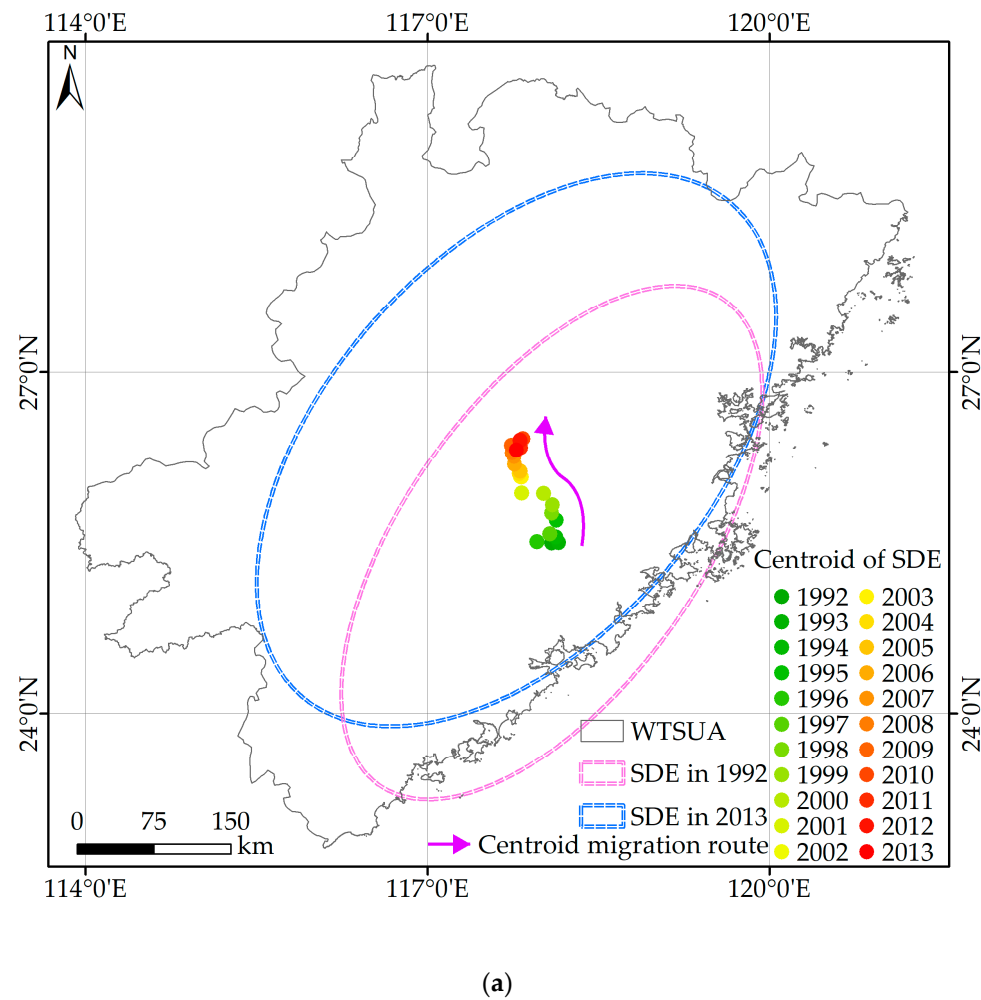


Figure 3. Spatio-temporal dynamics of standard deviation ellipse (SDE) elements for urban areas from 1992 to 2013. (a) spatial distribution and centroid migration route of SDE from 1992 to 2013; (b) areal change trend of SDE spatial distribution from 1992 to 2013; (c) azimuth change of SDE from 1992 to 2013.

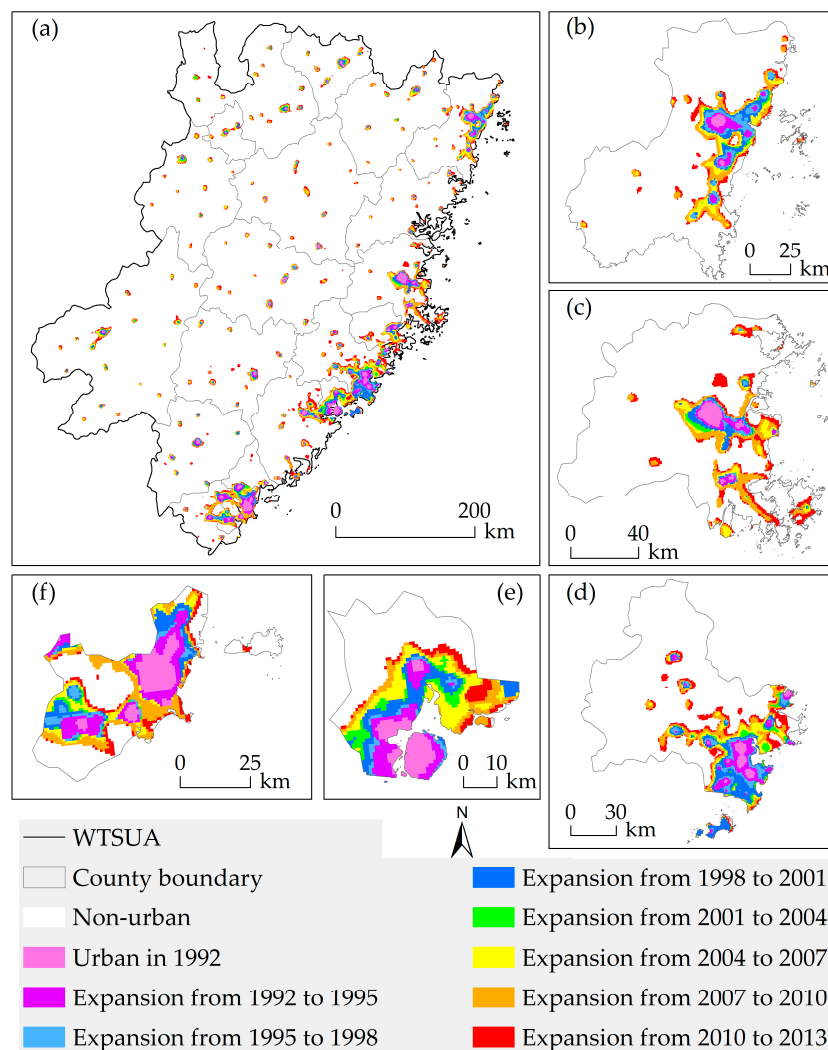


Figure 4. Spatio-temporal sprawl pattern of the WTSUA from 1992 to 2013. (a) spatio-temporal distribution of urban areas of the WTSUA from 1992 to 2013; (b) expansion dynamics of urban areas in Wenzhou city; (c) expansion dynamics of urban areas in Fuzhou city; (d) expansion dynamics of urban areas in Quanzhou city; (e) expansion dynamics of urban areas in Xiamen city; (f) expansion dynamics of urban areas in Shantou city.

3.1.3. City Rank-Size Distribution Change of Urban Agglomeration System

The urban rank-size distribution dynamics are shown in Figure 5. The value of the estimated Pareto coefficient ranged from 0.58 to 0.78, indicating an uneven city size distribution in the WTSUA, namely, there were a small number of large-sized cities. According to the temporal change of the Pareto coefficient, three different stages were defined: 1992–2000, 2001–2009, and 2009–2013. From 1992 to 2000, despite some small fluctuations, the Pareto coefficient increased, indicating that more nonuniformities had occurred during this stage. From 2001 to 2009, the Pareto coefficient experienced a general decrease. It can be inferred that during this period, WTSUA's cities experienced a “balancing trend”, with large-sized cities growing more slowly and decreasing in rank, while small-sized cities grew more rapidly and increased in rank. From 2010 to 2013, the Pareto coefficient was basically stable with a lower value, suggesting a more balanced distribution of urban rank-size than the previous two stages.

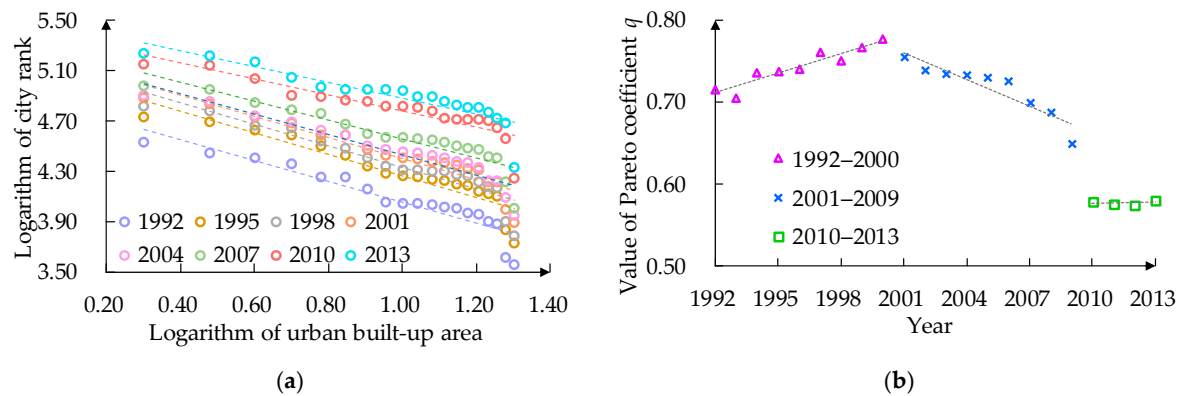


Figure 5. Temporal changes of the urban rank-size distribution and Pareto coefficient (q) in the WTSUA from 1992 to 2013. (a) change trend of the urban rank-size distribution; (b) change trend of Pareto coefficient (q).

3.2. Urbanization Quality of Urban Agglomeration

The weight of each indicator for the urbanization quality evaluation system was calculated by the EW model shown in Figure 6. It indicated that econo-demographic development accounted for the largest weight (42.34%), followed by social well-being level (36.18%). Eco-environment status was the smallest weight (20.58%) in the first-grade indices. In terms of the basic indices, their weight was roughly similar.

Figure 7 illustrates the urbanization quality dynamics of the WTSUA. A progressive increase trend was shown for the urbanization quality of each city from 1992–2013. Among different subsystems of urbanization quality, econo-demographic development changed most dramatically, with an increase of 1402.86% during the study period. The social well-being level and eco-environment status increased by 78.80% and 98.69% from 1992 to 2013, respectively.

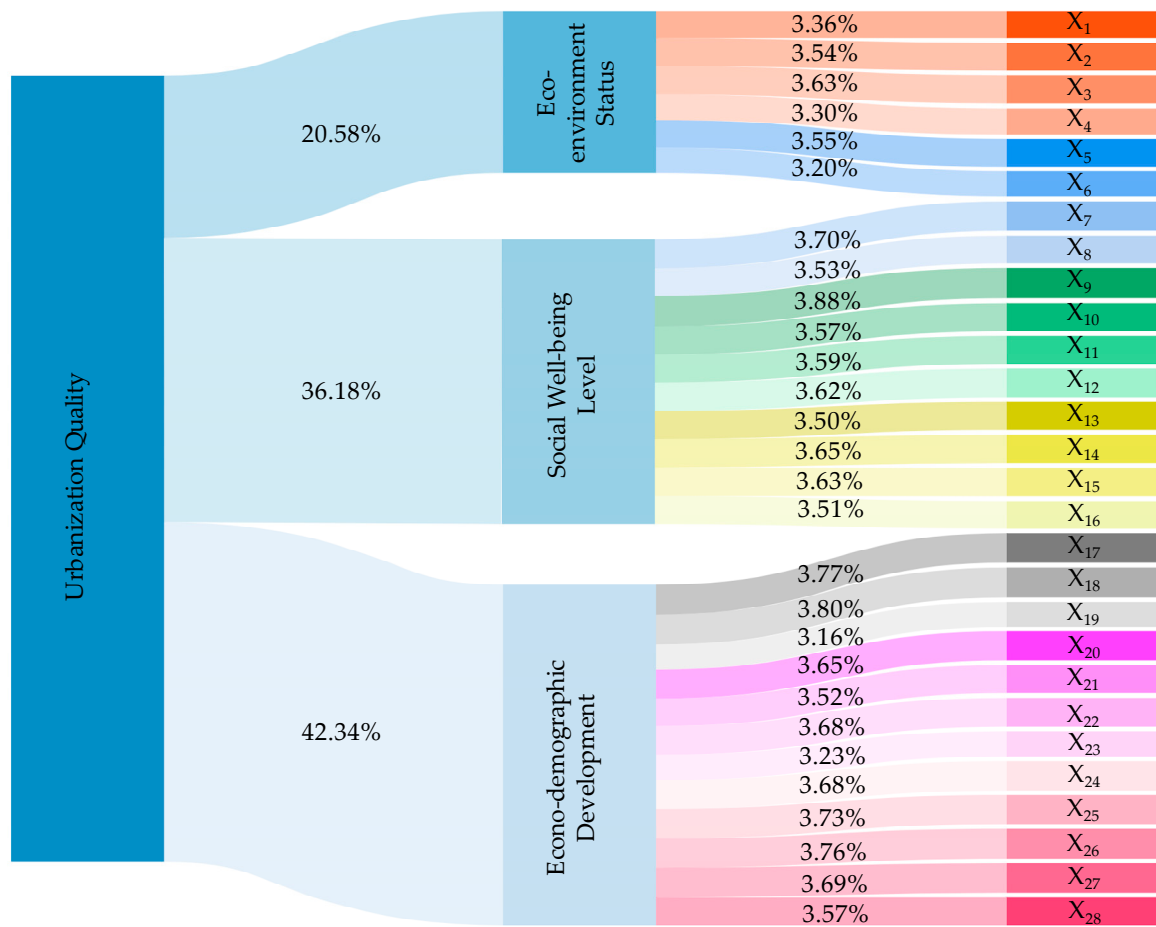


Figure 6. Weight of each indicator for the urbanization quality evaluation system ((X₁: Per capita water resources, X₂: Per capita land area, X₃: Per capita gas supply volume, X₄: Per capita green areas, X₅: Domestic sewage treatment rate, X₆: Landfill rate for urban waste, X₇: Proportion of built-up area and total area, X₈: Per capita urban road area in municipal district, X₉: Per capita public library holdings, X₁₀: Proportion of educational expenditure to GDP, X₁₁: Proportion of science and technology expenditure to GDP, X₁₂: Number of teachers per 10,000 students, X₁₃: Number of medical beds per 10,000 persons, X₁₄: Number of buses per 10,000 persons, X₁₅: Per capita housing, X₁₆: Registered urban unemployment rate, X₁₇: Proportion of population in municipal district to total population, X₁₈: Population density in municipal district, X₁₉: Proportion of secondary and tertiary industry employment to total employment, X₂₀: Per capita investment in fixed assets, X₂₁: Per capita GDP, X₂₂: GDP, X₂₃: Per capita GDP in the secondary and tertiary industry, X₂₄: Per capita disposable income of urban residents, X₂₅: Per capita local government fiscal revenue, X₂₆: Proportion of secondary and tertiary industry GDP to total GDP, X₂₇: Total retail sales of consumer goods, X₂₈: Deposits of financial institutions at year-end).

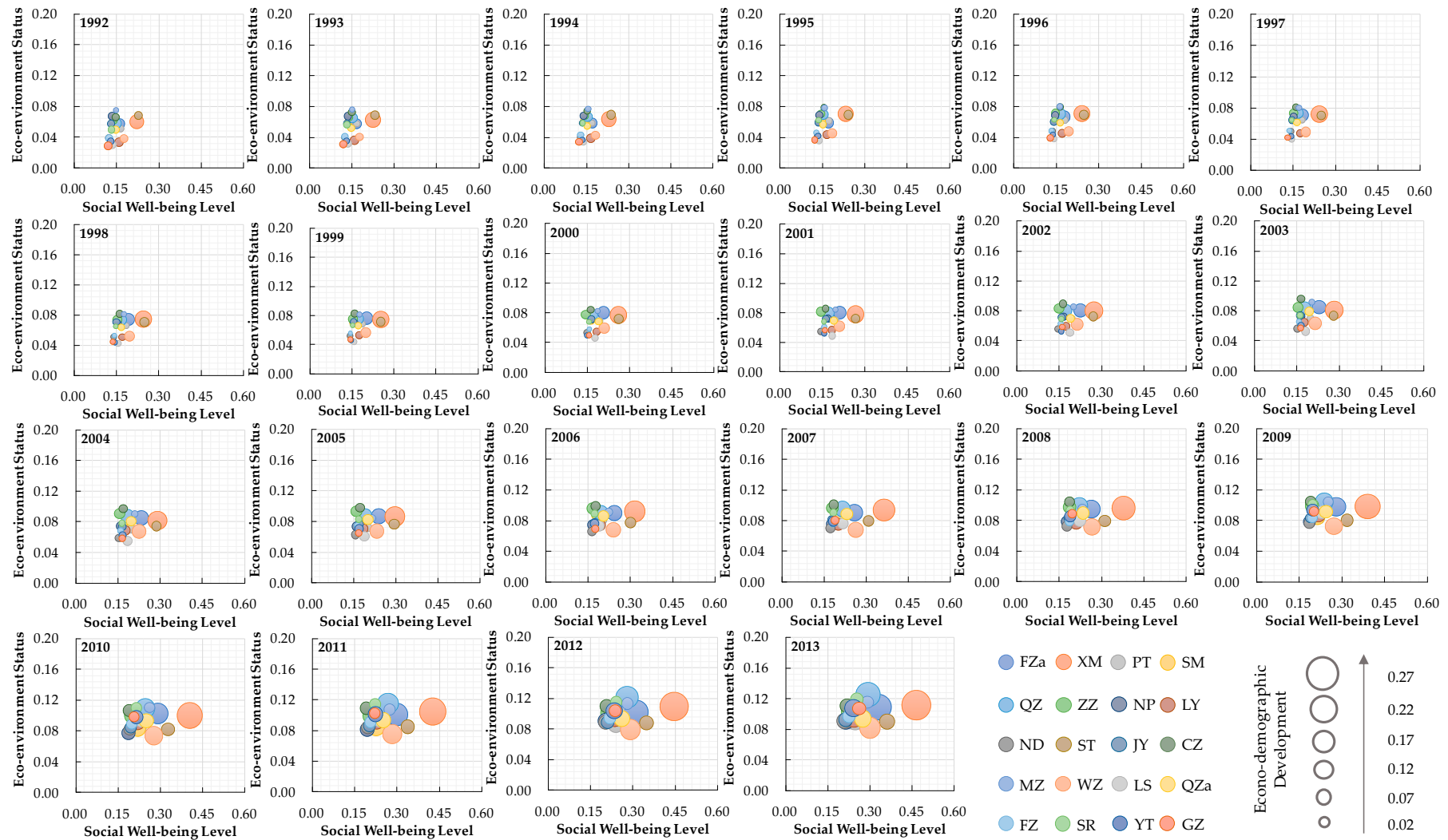


Figure 7. Urbanization quality evolution of the WTSUA from 1992 to 2013.

3.3. Coupling Coordination Relationship between Urban Sprawl and Urbanization Quality

Figure 8 visualizes the spatio-temporal dynamics of the coupling coordination relationship between urbanization quality and urban sprawl for the WTSUA from 1992 to 2013. During the study period, the level of coupling coordination increased gradually for each city. Moreover, the CCD value of the central-western inland areas was obviously lower than that of the eastern coastal regions, showing a significant spatial variation (Figure 8a). As for the total WTSUA, the value of the CCD presented a gradual increase over time, suggesting the enhancement of improving coordination between urban sprawl and urbanization quality from 1992 to 2013 (Figure 8b). Specifically, the coupling coordination level of urban sprawl and urbanization quality experienced four stages: a serious incoordination phase (low coupling state) from 1992–1994, a moderate incoordination phase (low coupling state) from 1995–2005, a slight incoordination phase (antagonism state) from 2006–2009, and a basic coordination phase (running-in state) from 2010–2013. It is noteworthy that although the overall coupling coordination level of the study area was basic coordination by 2013, the coupling coordination relationship between urban sprawl and urbanization quality had developed into moderate coordination or high coordination stage in some eastern coastal cities.

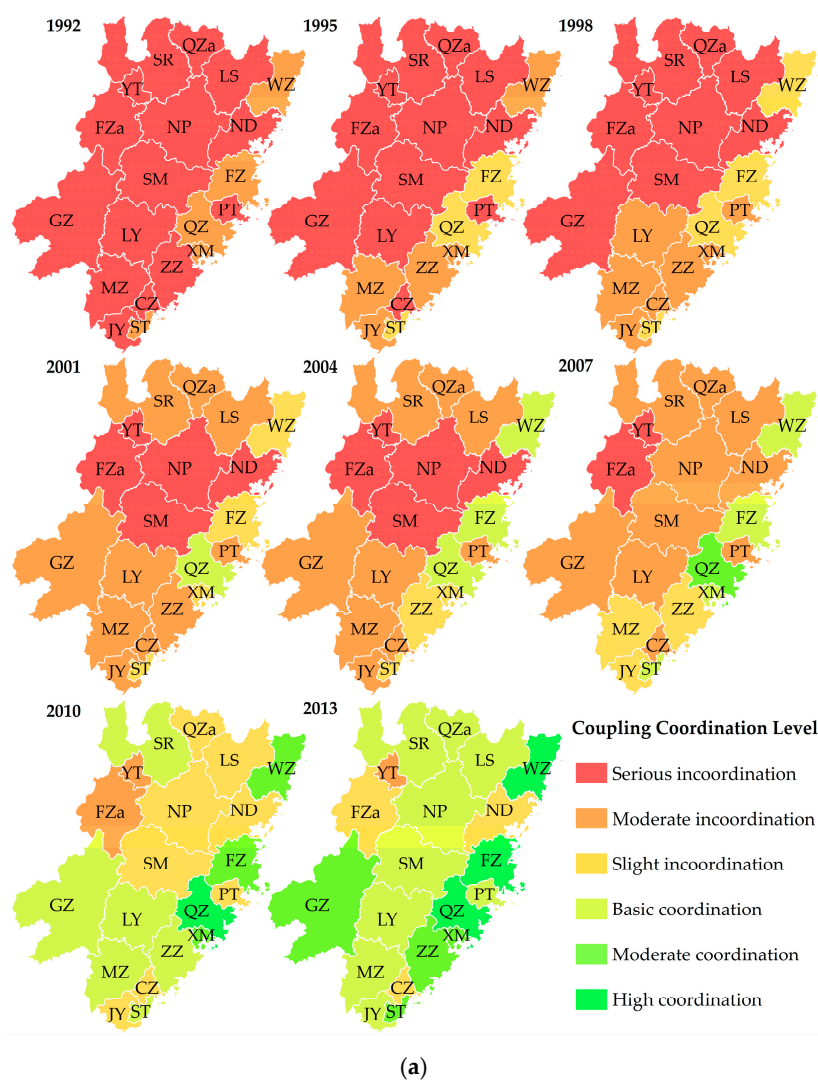


Figure 8. Cont.

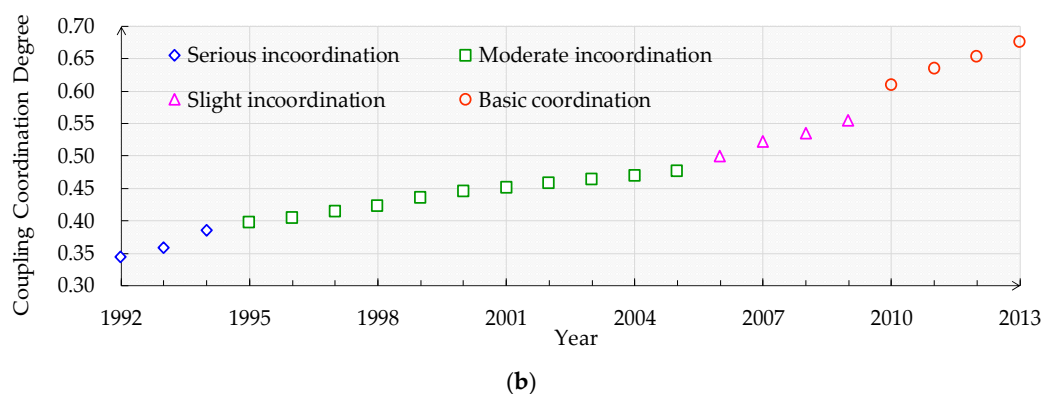


Figure 8. Spatio-temporal dynamics of coupling coordination level between urbanization quality and urban sprawl for the WTSUA from 1992 to 2013. (a) spatial variations of coupling coordination level between urbanization quality and urban sprawl for the WTSUA in different years; (b) change trend of CCD between urbanization quality and urban sprawl for the entire WTSUA from 1992 to 2013.

4. Discussion

4.1. Urban Development Associated with State-Led Policies and Market-Oriented Land Reform

Urban areas, considered as the core centers of social and economic development, are crucial for ensuring national stabilization and people's livelihoods. Since the implementation of 'Reform and Opening-up', China has experienced rapid urbanization [62,63]. The ratio of urbanization was less than 18% in 1978 but up to 36% in 2000; it will be more than 80% by 2050 [8]. In this context, the urban system has driven unprecedented development, accompanied by urban spatial expansion and improvements in the urban structure. In the WTSUA, our results suggest that the distribution and expansion speed of urban areas have increased, with a rise of 1602.86% from 1992 to 2013 (Figures 2 and 3, and Table 4). Previous studies in China concerning the urban sprawl dynamics in Beijing, Shanghai, Guangzhou, and Wuhan show that these cities present a similar trend of urban expansion [64–67]. In the process of rapid urban expansion, a series of issues associated with the eco-environment and society have arisen [68–70]. Facing the challenges of urban sprawl, several plans and policies have been promulgated to promote coordinated urban development. Figure 9 illustrates the characteristics, emphasis, and pivotal policies and events in the different urban sprawl stages of China. It shows that the guiding principles of national urban development were issued and implemented in the early 1980s, which aimed to regulate orderly urban development by actively developing small-sized cities, slowly developing medium-sized cities, and controlling the scale of large-sized cities [62]. Driven by these policies, small- and medium-sized cities have developed rapidly. This probably explains why the expansion speed of the noncentral cities of the WTSUA was higher than that of the central cities, and why the centroid of urban areas shifted towards noncentral cities from 1992 to 2013. Through the government's macro-control of urban development, more people have migrated to small- and medium-sized cities, which alleviates, to a certain extent, the eco-environmental and social pressures caused by excessive population growth in large-sized cities. Meanwhile, owing to the gradual elimination of the rural and urban household registration system since 1997 [71], people migrating from rural to urban areas can obtain more and better social welfare and benefits than before. Our research found that econo-demographic development elevated dramatically, with an increase of 1402.86%, and the social well-being level increased by 78.80% in the WTSUA from 1992 to 2013. This has contributed to the promotion of social stability in urban areas while stimulating urban sprawl. In 2006, the Chinese government issued a new General Land Use Plan (2006–2020) and strengthened its control over the scale of urban areas in large-sized cities [72]. Moreover, as eco-environmental issues have become more widely recognized, a variety of environmental conservation policies and plans have been introduced to improve the eco-environment of urban systems [73]. As observed from

our findings, the eco-environment status increased by 98.69%, the urbanization quality exhibited an upward trend, and the coupling coordination level between urbanization quality and urban sprawl increased gradually from 1990 to 2013 (Figures 7 and 8). A previous study also stated that high-levels of economy, eco-environment, and social well-being would be conducive to achieving the desired effects of urban sprawl and ameliorating the quality of urbanization [4], which is consistent with our research.

In addition to national policies, several regional urban planning schemes are also indirectly or directly responsible for the urban expansion and urbanization quality of the WTSUA. In 1992, Fujian Province's government formulated a development strategy aiming at accelerating the economic progress of the southeast coastal zone [74]. Thus, the central cities situated in the coastal zone were given priority for development driven by this policy, resulting in a gradual increase in the differentiation of rank-size distribution between central cities and noncentral cities. In 2001, the separation system of urban and rural household registration was abolished, which led to a further migration wave of rural people into different sized cities [75]. With the rapid development of small- and medium-sized cities, the disparities in rank-size distribution between central cities and noncentral cities declined. In 2009, the WTSUA was formally established, which allowed systematic planning to better regulate urban sprawl; this also led to a more stable distribution of the city rank-size. Our findings showed that the change trend of the urban rank-size distribution of the WTSUA's cities could be divided into three stages, i.e., 1992–2000, 2001–2009, and 2010–2013 (Figure 5b), which was consistent with the time of regional policy implementation.

Market-oriented land reform is another common underlying force in the regulation of urban sprawl and urbanization quality; it is characterized by spontaneous institutional change induced by market-forces and initiated by private/nonstate sectors such as rural communities and township-village-enterprises [76]. On one hand, feasible land reform regulated by the market can effectively perfect the redistribution of land development power. Generally, the larger the city, the higher the commuting cost and land price, which can restrain the city's expansion and reduce urban sprawl. Notably, some empirical studies on large metropolitan areas proved that the top ten most compact cities are almost mega cities [77,78]. Under these circumstances, small- and medium-sized cities are more likely to have opportunities to expand, thereby optimizing the distribution of human, economic, and social resources. As referenced by Gao et al. [1], small- and medium-sized cities in China showed a more significant sprawl trend than large-sized cities from 1990 to 2010. On the other hand, compared with government intervention, market regulation is more rapid and flexible, and can respond to the process of urban expansion in a timely manner according to the current urban development situation. The market-driven mechanism can, thus, contribute to driving the urban sprawl pattern typified by the circle-layer structure, which seems to be a highly efficient method of urban development [12]. From 1992 to 2013, each city in the WTSUA was found to expand in a cycloid pattern.

As mentioned above, state-led planning and market-oriented land reform have played critical roles in regulating the urban space to accommodate the increasing demand for economic and population growth while promoting the social stability of the urban system. Consequently, this dual-driving force has resulted in a relatively high degree of urbanization quality.

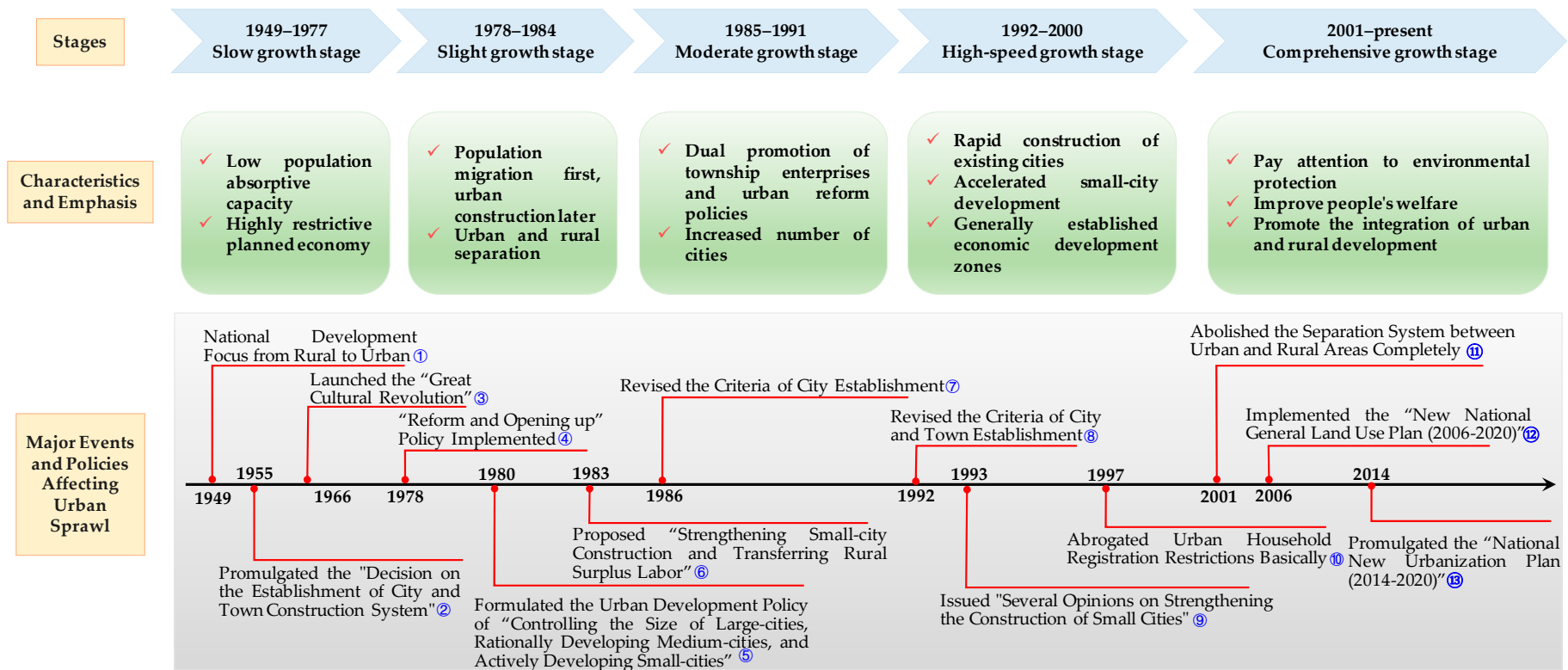


Figure 9. Characteristics, emphasis as well as major events and policies affecting urban sprawl in different stages of China (the major events and policies affecting urban sprawl are referenced by ① [79]; ② [80]; ③ [81]; ④ [63]; ⑤ [62]; ⑥ [82]; ⑦ [83]; ⑧ [84]; ⑨ [85]; ⑩ [71]; ⑪ [75]; ⑫ [72]; ⑬ [86]).

4.2. Lessons and Suggestions for WTSUA's Further Urban Planning

Although the coupling relationship between urban sprawl and urbanization quality of the WTSUA became more coordinated during the study period, there are still some issues that need to be addressed. With regard to central cities and noncentral cities, there were distinct spatial differences between them in urban expansion intensity and the coupling coordination level between urban sprawl and urbanization quality (Table 4, Figures 3, 4 and 8). For the central cities, the urban expansion rate was low but the coupling coordination level was high, while for the noncentral cities, the opposite pattern was observed, implying that the urban development in the eastern coastal and central-western areas has not been balanced. Furthermore, with continuing urban expansion, cities, especially large-sized cities, can be disrupted by many issues, such as population dilatation, resource depletion, environmental deterioration, traffic congestion, and housing shortages. In contrast, some small- and medium-sized cities have undergone slow economic development, population loss, and limited urban functionality [87]. Our findings showed that the eco-environment status and social well-being level count for about 60% of the urbanization quality for the WTSUA (Figure 6), indicating that the improvement of urbanization quality should pay more attention to eco-environment and social well-being. In addition, some land-use regulations and land reform arbitrarily segregate “rural” and “urban” land, which is not conducive to the integrated and coordinated development of rural and urban areas [88].

According to the results of this study, some suggestions can be proposed to guide the formulation and implementation of sustainable urban development planning. First, the government should propose more feasible policies and measures to strictly limit the expansion of large-sized cities and encourage the development of small- and medium-sized cities. Decision-makers and scientists should develop more effective plans to solve city problems and stop the uncontrolled expansion of urban areas. Second, it is necessary to establish an effective mechanism for the government to intervene reasonably in the market economy, which would avoid or reduce the further deterioration of city functions. Third, the “*Desakota*” regions, referred to as areas with an intense mixture of nonagricultural and agricultural activities that often stretch along corridors between large-sized city centers, should be the focus of attention, because the development processes of these regions will directly or indirectly influence urban sprawl [89]. Fourth, eco-environmental conservation and social welfare should be continued to be reinforced and improved by promulgating related plans and regulations, with the aim of achieving regional sustainable development. Fifth, existing effective urban sprawl patterns should be used as a reference in future urban planning.

4.3. Advantages and Limitations of the Study

Previous studies have focused on the relationship between urban sprawl and some attributes involved in urban development, such as revenue, pollution, land-use change, and population migration. Nevertheless, urban areas form large-scale complex systems, which not only have their own, inherent elements, but are also closely associated with other open ecosystems. Therefore, it may be difficult to discern the elements of urban development thoroughly by focusing only on one or a few correlative factors of urban sprawl. In our study, urbanization quality was assessed comprehensively, and the coupling relationship between urban sprawl and urbanization quality was quantified systemically. This will improve our understanding of the causal relationship between these parameters.

The efficient and accurate determination of indicator weight is crucial to the evaluation process and result. Due to the differentiation of diverse regions in terms of resource endowment, development policy, and technology level, the weight of each indicator in the evaluation system would vary from region to region for the urbanization quality. Hence, based on the subjective weight methods, it could be difficult to obtain unbiased results if the expert lacks a systemic understanding of the study area. However, the EM model used in the research, as an objective weight approach, not only eliminates the influence of the subjectivity of experts and the differences of evaluated objects, but also reduces the time spent establishing an expert panel [9,18]. Therefore, the weight approach adopted in the study

has a certain applicability and advantages in assessing urbanization quality in the WTSUA and even in other regions.

Many studies involving urban area extraction have used traditional optical remote sensing images as the basic data sources. However, the processing of information based on these data are more often than not time-consuming, especially for some large-scale study areas. Moreover, in previous studies, the thresholds of urban area extraction based on nighttime light data were usually determined by subjective judgment or with the aid of auxiliary data, which would be not accurate enough and omit some urban area information [28]. In contrast, the long-term urban patches in our study were automatically identified by a thresholding approach, i.e., the OTSU method, which was more effective, labor-saving, and precise. Furthermore, the frequency of DMSP/OLS nighttime light observations is greater, making it possible to detect the dynamic trends of urban sprawl and undertake in-depth analyses of the driving mechanisms of urban sprawl at a regional scale.

Image resolution is a pivotal prerequisite for geo-object recognition, as it largely determines the ability to identify different objects. However, because of its low spatial resolution, DMSP/OLS nighttime light imagery may not reflect urban information well at a small-scale. As a result, a loss of precision might occur when extracting details of small urban areas. Thus, it is imperative to improve the resolution of the DMSP/OLS nighttime light data by using high-resolution optical images in future research. In addition, other limitations existed in the time-series DMSP/OLS nighttime light images. The nighttime light information recorded on the DMSP/OLS dataset only became available in 1992, and has been unavailable since 2014, leading to a lack of data for the study of the urban dynamics of previous and more recent years. Therefore, it is necessary that a longer time series dataset be formed by fusing multisource night light data; this would be conducive to more scientific and reasonable analyses of the dynamics of urban expansion.

5. Conclusions

Analyses and assessments of urban sprawl and urbanization quality for urban agglomerations are essential for defining the urban sprawl dynamics, understanding the reciprocal relationship between urban sprawl and urbanization quality, and underpinning knowledge-based urban development planning. In the study, taking the DMSP/OLS dataset as the basic data source, the spatio-temporal dynamics of urban areas were determined using the UERI, SDE model, and a RSR model for the WTSUA from 1992 to 2013. Based on an EW model and a CCD model, the urbanization quality and the coupling coordination level between urban sprawl and urbanization quality were evaluated and quantified, respectively. Our results showed that the urban areas experienced a significant increase in a cycloid expansion pattern, and that their rank-size distribution was uneven and changed as a result of the implementation of different policies. As urbanization quality increased, the coupling relationship between urban sprawl and urbanization quality gradually increased from serious incoordination to basic coordination. Two main driving forces, i.e., state-led policies and market-oriented land reform, played crucial roles in promoting the coupling coordination development between urbanization quality and urban sprawl in the WTSUA. These results could improve our understanding of urban sprawl dynamics and their coupling relationship with urbanization quality. These conclusions can be used as a guide to effectively facilitate orderly urban expansion and urbanization quality improvement.

Author Contributions: Conceptualization, methodology, validation, formal analysis, writing—original draft preparation, supervision, project administration, and funding acquisition, C.L.; writing—review and editing, L.L. and C.R.; investigation, resources, and data curation, Y.L., Y.S., and Y.H.; visualization, Y.C. and S.L.; software, W.F. All authors have read and agreed to the published version of the manuscript.

Funding: This research was jointly funded by the Social Science and Humanity on Young Fund of the Ministry of Education of China (No. 17YJCZH118), the Program of China Scholarship Council (201907870005), and the Scientific Research Project on Outstanding Young of the Fujian Agriculture and Forestry University (No. XJQ201920).

Acknowledgments: We appreciate the geospatial data provide by the Northeast Branch of National Earth System Science Data Center of China.

Conflicts of Interest: The authors declare no conflict of interest.

References

1. Gao, B.; Huang, Q.; He, C.; Sun, Z.; Zhang, D. How does sprawl differ across cities in China? A multi-scale investigation using nighttime light and census data. *Landsc. Urban Plan.* **2016**, *148*, 89–98. [\[CrossRef\]](#)
2. Koprowska, K.; Łaskiewicz, E.; Kronenberg, J. Is urban sprawl linked to green space availability? *Ecol. Indic.* **2020**, *108*, 105723. [\[CrossRef\]](#)
3. Jiang, G.; Ma, W.; Wang, D.; Zhou, D.; Zhang, R.; Tao, Z. Identifying the internal structure evolution of urban built-up land sprawl (UBLS) from a composite structure perspective: A case study of the Beijing metropolitan area, China. *Land Use Policy* **2017**, *62*, 258–267.
4. Chen, D.L.; Lu, X.H.; Liu, X.; Wang, X. Measurement of the eco-environmental effects of urban sprawl: Theoretical mechanism and spatiotemporal differentiation. *Ecol. Indic.* **2019**, *105*, 6–15. [\[CrossRef\]](#)
5. Liang, Y.; Lu, W.; Wu, W. Are social security policies for Chinese landless farmers really effective on health in the process of Chinese rapid urbanization? A study on the effect of social security policies for Chinese landless farmers on their health-related quality of life. *Int. J. Equity Health* **2014**, *13*, 5. [\[CrossRef\]](#)
6. Lan, F.; Da, H.; Wen, H.; Wang, Y. Spatial structure evolution of urban agglomerations and its driving factors in mainland china: From the monocentric to the polycentric dimension. *Sustainability* **2019**, *11*, 610. [\[CrossRef\]](#)
7. Ning, Y. *Issues in China's Urban Agglomeration Studies and New Exploration for China's Urban Agglomeration Selection and Nurturing*; Science Press: Beijing, China, 2015.
8. Fang, C.; Yu, D. Urban agglomeration: An evolving concept of an emerging phenomenon. *Landsc. Urban Plan.* **2017**, *162*, 126–136. [\[CrossRef\]](#)
9. Zhou, D.; Xu, J.; Wang, L.; Lin, Z. Assessing urbanization quality using structure and function analyses: A case study of the urban agglomeration around Hangzhou Bay (UAHB), China. *Habitat Int.* **2015**, *49*, 165–176. [\[CrossRef\]](#)
10. Tian, L.; Ge, B.; Li, Y. Impacts of state-led and bottom-up urbanization on land use change in the peri-urban areas of Shanghai: Planned growth or uncontrolled sprawl? *Cities* **2017**, *60*, 476–486. [\[CrossRef\]](#)
11. Nijkamp, P.; Perrels, A. *Sustainable Cities in Europe*, 1st ed.; Routledge: London, UK, 2018. [\[CrossRef\]](#)
12. Jiang, G.H.; Ma, W.Q.; Qu, Y.B.; Zhang, R.J.; Zhou, D.Y. How does sprawl differ across urban built-up land types in China? A spatial-temporal analysis of the Beijing metropolitan area using granted land parcel data. *Cities* **2016**, *58*, 1–9. [\[CrossRef\]](#)
13. Bagheri, B.; Tousi, S.N. An explanation of urban sprawl phenomenon in Shiraz Metropolitan Area (SMA). *Cities* **2018**, *73*, 71–90. [\[CrossRef\]](#)
14. Liu, Y.; Fan, P.; Yue, W.; Song, Y. Impacts of land finance on urban sprawl in China: The case of Chongqing. *Land Use Policy* **2018**, *72*, 420–432. [\[CrossRef\]](#)
15. Dadashpoor, H.; Salarian, F. Urban sprawl on natural lands: Analyzing and predicting the trend of land use changes and sprawl in Mazandaran city region, Iran. *Environ. Dev. Sustain.* **2020**, *22*, 593–614. [\[CrossRef\]](#)
16. Hatab, A.A.; Cavinato, M.E.R.; Lindemer, A.; Lagerkvist, C.J. Urban sprawl, food security and agricultural systems in developing countries: A systematic review of the literature. *Cities* **2019**, *94*, 129–142. [\[CrossRef\]](#)
17. Pan, J. From industrial toward ecological in China. *Science* **2012**, *336*, 1397. [\[CrossRef\]](#) [\[PubMed\]](#)
18. Wang, Y.; Li, X.; Kang, Y.; Chen, W.; Zhao, M.; Li, W. Analyzing the impact of urbanization quality on CO₂ emissions: What can geographically weighted regression tell us? *Renew. Sustain. Energy Rev.* **2019**, *104*, 127–136. [\[CrossRef\]](#)
19. Liu, Z.; Liu, S.; Qi, W.; Jin, H. Urban sprawl among Chinese cities of different population sizes. *Habitat Int.* **2018**, *79*, 89–98. [\[CrossRef\]](#)
20. Lin, X.; Lu, C.; Song, K.; Su, Y.; Lei, Y.; Zhong, L.; Gao, Y. Analysis of coupling coordination variance between urbanization quality and eco-environment pressure: A case study of the west taiwan strait urban agglomeration, China. *Sustainability* **2020**, *12*, 2643. [\[CrossRef\]](#)
21. Martinez-Zarzoso, I. The impact of urbanization on CO₂ emissions: Evidence from developing countries. *Ecol. Econ.* **2011**, *70*, 1344–1353. [\[CrossRef\]](#)

22. Jat, M.K.; Garg, P.K.; Khare, D. Monitoring and modelling of urban sprawl using remote sensing and GIS techniques. *Int. J. Appl. Earth Obs.* **2008**, *10*, 26–43. [[CrossRef](#)]
23. Shahtahmassebi, A.R.; Song, J.; Zheng, Q.; Blackburn, G.A.; Wang, K.; Huang, L.Y.; Pan, Y.; Moore, N.; Shahtahmassebi, G.; Haghighi, R.S.; et al. Remote sensing of impervious surface growth: A framework for quantifying urban expansion and re-densification mechanisms. *Int. Appl. Earth Obs.* **2016**, *46*, 94–112. [[CrossRef](#)]
24. Sonde, P.; Balamwar, S.; Ochawar, R.S. Urban sprawl detection and analysis using unsupervised classification of high resolution image data of Jawaharlal Nehru Port Trust area in India. *Remote Sens. Appl. Soc. Environ.* **2020**, *17*, 100282. [[CrossRef](#)]
25. Rahman, A.; Aggarwal, S.P.; Netzband, M.; Fazal, S. Monitoring urban sprawl using remote sensing and GIS techniques of a fast growing urban center, India. *IEEE J. Sel. Top. Appl. Earth Obs. Remote Sens.* **2010**, *4*, 56–64. [[CrossRef](#)]
26. Kantakumar, L.N.; Kumar, S.; Schneider, K. Spatiotemporal urban expansion in Pune metropolis, India using remote sensing. *Habitat Int.* **2016**, *51*, 11–22. [[CrossRef](#)]
27. Yang, C.; Li, Q.; Hu, Z.; Chen, J.; Shi, T.; Ding, K.; Wu, G. Spatiotemporal evolution of urban agglomerations in four major bay areas of USA, China and Japan from 1987 to 2017: Evidence from remote sensing images. *Sci. Total Environ.* **2019**, *671*, 232–247. [[CrossRef](#)]
28. Liu, Z.; He, C.; Zhang, Q.; Huang, Q.; Yang, Y. Extracting the dynamics of urban expansion in China using DMSP-OLS nighttime light data from 1992 to 2008. *Landsc. Urban Plan.* **2012**, *106*, 62–72. [[CrossRef](#)]
29. Elvidge, C.D.; Ziskin, D.; Baugh, K.E.; Tuttle, B.T.; Ghosh, T.; Pack, D.W.; Erwin, E.H.; Zhizhin, M. A fifteen year record of global natural gas flaring derived from satellite data. *Energies* **2009**, *2*, 595–622. [[CrossRef](#)]
30. Zhou, Y.; Li, X.; Asrar, G.R.; Smith, S.J.; Imhoff, M. A global record of annual urban dynamics (1992–2013) from nighttime lights. *Remote Sens. Environ.* **2018**, *219*, 206–220. [[CrossRef](#)]
31. Small, C.; Pozzi, F.; Elvidge, C.D. Spatial analysis of global urban extent from DMSP-OLS night lights. *Remote Sens. Environ.* **2005**, *96*, 277–291. [[CrossRef](#)]
32. Zhong, Y.; Lin, A.; He, L.; Zhou, Z.; Yuan, M. Spatiotemporal dynamics and driving forces of urban land-use expansion: A case study of the yangtze river economic belt, China. *Remote Sens.* **2020**, *12*, 287. [[CrossRef](#)]
33. Castells-Quintana, D. Malthus living in a slum: Urban concentration, infrastructure and economic growth. *J. Urban Econ.* **2017**, *98*, 158–173. [[CrossRef](#)]
34. Li, D.R.; Yu, H.R.; Li, X. The spatial-temporal pattern analysis of city development in countries along the belt and road initiative based on nighttime light data. *Geomat. Inform. Sci. Wuhan Univ.* **2017**, *42*, 711–720.
35. Huang, Q.; He, C.; Gao, B.; Yang, Y.; Liu, Z.; Zhao, Y.; Dou, Y. Detecting the 20 year city-size dynamics in China with a rank clock approach and DMSP/OLS nighttime data. *Landsc. Urban Plan.* **2015**, *137*, 138–148. [[CrossRef](#)]
36. Stokes, E.C.; Seto, K.C. Characterizing urban infrastructural transitions for the Sustainable Development Goals using multi-temporal land, population, and nighttime light data. *Remote Sens. Environ.* **2019**, *234*, 111430. [[CrossRef](#)]
37. Zhang, Q.; Seto, K.C. Mapping urbanization dynamics at regional and global scales using multi-temporal DMSP/OLS nighttime light data. *Remote Sens. Environ.* **2011**, *115*, 2320–2329. [[CrossRef](#)]
38. Li, X.; Elvidge, C.; Zhou, Y.; Cao, C.; Warner, T. Remote sensing of night-time light. *Int. J. Remote Sens.* **2017**, *38*, 5855–5859. [[CrossRef](#)]
39. Guo, Q.H.; Zhang, G.Q.; Cui, S.H. The characteristics in urbanization of economic region on west coast of Taiwan Strait. *Econ. Geogr.* **2009**, *29*, 907–912.
40. Hu, X.; Qian, Y.; Pickett, S.T.; Zhou, W. Urban mapping needs up-to-date approaches to provide diverse perspectives of current urbanization: A novel attempt to map urban areas with nighttime light data. *Landsc. Urban Plan.* **2020**, *195*, 103709. [[CrossRef](#)]
41. Zhang, C.; Pei, Y.; Li, J.; Qin, Q.; Yue, J. Application of luojia 1-01 nighttime images for detecting the light changes for the 2019 spring festival in western cities, China. *Remote Sens.* **2020**, *12*, 1416. [[CrossRef](#)]
42. Guk, E.; Levin, N. Analyzing spatial variability in night-time lights using a high spatial resolution color Jilin-1 image—Jerusalem as a case study. *ISPRS J. Photogramm.* **2020**, *163*, 121–136. [[CrossRef](#)]
43. City Application of Jilin 1 Nighttime Light Data. Available online: <https://xw.qq.com/cmsid/20191110A04ICV00> (accessed on 11 November 2019).

44. Li, X.; Li, X.; Li, D.; He, X.; Jendryke, M. A preliminary investigation of LuoJia-1 night-time light imagery. *Remote Sens. Lett.* **2019**, *10*, 526–535. [\[CrossRef\]](#)
45. Otsu, N. A threshold selection method from gray-level histograms. *IEEE Trans. Syst. Man Cybern.* **1979**, *9*, 62–66. [\[CrossRef\]](#)
46. Ma, L.; Li, M.; Gao, Y.; Chen, T.; Ma, X.; Qu, L. A novel wrapper approach for feature selection in object-based image classification using polygon-based cross-validation. *IEEE Geosci. Remote Sens. Soc.* **2017**, *14*, 409–413. [\[CrossRef\]](#)
47. Ma, Y.; Xu, R. Remote sensing monitoring and driving force analysis of urban expansion in Guangzhou City, China. *Habitat Int.* **2010**, *34*, 228–235. [\[CrossRef\]](#)
48. Wachowicz, M.; Liu, T. Finding spatial outliers in collective mobility patterns coupled with social ties. *Int. J. Geogr. Inf. Sci.* **2016**, *30*, 1806–1831. [\[CrossRef\]](#)
49. Wang, B.; Shi, W.; Miao, Z. Confidence analysis of standard deviational ellipse and its extension into higher dimensional Euclidean space. *PLoS ONE* **2015**, *10*, e0118537. [\[CrossRef\]](#)
50. Du, Q.; Zhou, J.; Pan, T.; Sun, Q.; Wu, M. Relationship of carbon emissions and economic growth in China's construction industry. *J. Clean. Prod.* **2019**, *220*, 99–109. [\[CrossRef\]](#)
51. Živanović, Z.; Tošić, B.; Nikolić, T.; Gatarić, D. Urban System in Serbia-the Factor in the Planning of Balanced Regional Development. *Sustainability* **2019**, *11*, 4168. [\[CrossRef\]](#)
52. Ho, W. Integrated analytic hierarchy process and its applications-a literature review. *Eur. J. Oper. Res.* **2007**, *186*, 211–228. [\[CrossRef\]](#)
53. Musa, H.D.; Yacob, M.R.; Abdullah, A.M.; Ishak, M.Y. Delphi method of developing environmental well-being indicators for the evaluation of urban sustainability in Malaysia. *Procedia Environ. Sci.* **2015**, *30*, 244–249. [\[CrossRef\]](#)
54. Ho, C.T.B.; Wu, D.D. Online banking performance evaluation using data envelopment analysis and principal component analysis. *Comput. Oper. Res.* **2009**, *36*, 1835–1842.
55. Adamowski, J.; Chan, H.F.; Prasher, S.O.; OzgaeZielinski, B.; Sliusarieva, A. Comparison of multiple linear and nonlinear regression, autoregressive integrated moving average, artificial neural network, and wavelet artificial neural network methods for urban water demand forecasting in montreal, Canada. *Water Resour. Res.* **2012**, *48*, W01528. [\[CrossRef\]](#)
56. Qi, Z.; Ye, X.; Zhang, H.; Yu, Z. Land fragmentation and variation of ecosystem services in the context of rapid urbanization: The case of Taizhou city, China. *Stoch. Environ. Res. Risk A.* **2014**, *28*, 843–855. [\[CrossRef\]](#)
57. Tian, Z.P.; Zhang, H.Y.; Wang, J.; Wang, J.Q.; Chen, X.H. Multi-criteria decision-making method based on a cross-entropy with interval neutrosophic sets. *Int. J. Syst. Sci.* **2016**, *47*, 3598–3608. [\[CrossRef\]](#)
58. Li, Y.; Li, D. Assessment and forecast of Beijing and Shanghai's urban ecosystem health. *Sci. Total Environ.* **2014**, *487*, 154–163. [\[CrossRef\]](#)
59. Xing, L.; Xue, M.; Hu, M. Dynamic simulation and assessment of the coupling coordination degree of the economy–resource–environment system: Case of Wuhan City in China. *J. Environ. Manag.* **2019**, *230*, 474–487.
60. Shi, T.; Yang, S.; Zhang, W.; Zhou, Q. Coupling coordination degree measurement and spatiotemporal heterogeneity between economic development and ecological environment-empirical evidence from tropical and subtropical regions of China. *J. Clean. Prod.* **2020**, *244*, 118739. [\[CrossRef\]](#)
61. Wen, H.; Wen, F. Coupling and coordination analysis of water resources-economy ecological environment in key provinces of “the Belt and Road”. *Eng. J. Wuhan Univ.* **2019**, *52*, 870–877.
62. Chen, M.; Liu, W.; Tao, X. Evolution and assessment on China's urbanization 1960–2010: Under-urbanization or over-urbanization? *Habitat Int.* **2013**, *38*, 25–33. [\[CrossRef\]](#)
63. Deng, F.F.; Huang, Y.Q. Uneven land reform and urban sprawl in China: The case of Beijing. *Prog. Plan.* **2004**, *61*, 211–236.
64. Yue, W.; Zhang, L.; Liu, Y. Measuring sprawl in large Chinese cities along the Yangtze river via combined single and multidimensional metrics. *Habitat Int.* **2016**, *57*, 43–52. [\[CrossRef\]](#)
65. Yu, X.J.; Ng, C.N. Spatial and temporal dynamics of urban sprawl along two urban–rural transects: A case study of Guangzhou, China. *Landsc. Urban Plan.* **2007**, *79*, 96–109. [\[CrossRef\]](#)
66. Yue, W.; Liu, Y.; Fan, P. Measuring urban sprawl and its drivers in large Chinese cities: The case of Hangzhou. *Land Use Policy* **2013**, *31*, 358–370. [\[CrossRef\]](#)
67. Jiang, F.; Liu, S.; Yuan, H.; Zhang, Q. Measuring urban sprawl in Beijing with geo-spatial indices. *J. Geogr. Sci.* **2007**, *17*, 469–478. [\[CrossRef\]](#)

68. Wigginton, N.S.; Fahrenkamp-Uppenbrink, J.; Wible, B.; Malakoff, D. Cities are the future. *Science* **2016**, *352*, 904–905. [CrossRef]
69. Foley, J.A.; DeFries, R.; Asner, G.P.; Barford, C.; Bonan, G.; Carpenter, S.R.; Helkowski, J.H. Global consequences of land use. *Science* **2005**, *309*, 570–574. [CrossRef]
70. Mao, D.; He, X.; Wang, Z.; Tian, Y.; Xiang, H.; Yu, H.; Man, W.; Jia, M.; Ren, C.; Zheng, H. Diverse policies leading to contrasting impacts on land cover and ecosystem services in Northeast China. *J. Clean. Prod.* **2019**, *240*, 117961. [CrossRef]
71. Li, T.; Ren, Y. The reform of *Hukou* system in Chinese cities and the social inclusion of floating population. *South China Popul.* **2011**, *26*, 17–24.
72. Chen, Y.; Chen, Z.; Xu, G.; Tian, Z. Built-up land efficiency in urban China: Insights from the general land use plan (2006–2020). *Habitat Int.* **2016**, *51*, 31–38. [CrossRef]
73. Zhang, K.M.; Wen, Z.G. Review and challenges of policies of environmental protection and sustainable development in China. *J. Environ. Manag.* **2008**, *88*, 1249–1261. [CrossRef]
74. Yi, X.N. Historical evolution and enlightenment of Fujian’s governance strategy since the founding of the People’s Republic of China. *Fujian Dangshi Yuekan* **2007**, *5*, 22–25.
75. State Council of the People’s Republic of China. Guanyu Jinyibu Tuijin Huji Zhidu Gaige de Yijian (Opinion on Further Advancing Reform of the Household Registration System). Available online: http://www.gov.cn/zhengce/content/2014-07/30/content_8944.htm (accessed on 30 July 2014).
76. Gu, S.; Li, Z. An institutional analysis of the process of urbanization in China from the bottom-up. *Soc. Sci. China* **2000**, *194*, 67–78.
77. Hamidi, S.; Ewing, R. A longitudinal study of changes in urban sprawl between 2000 and 2010 in the United States. *Landsc. Urban Plan.* **2014**, *128*, 72–82. [CrossRef]
78. Fulton, W.B.; Pendall, R.; Nguyen, M.; Harrison, A. *Who Sprawls Most? How Growth Patterns Differ Across the USA*; Brookings Institution, Center on Urban and Metropolitan Policy: Washington, DC, USA, 2001.
79. Gu, C.L.; Qiu, Y.L.; Ye, S.Z. Designation of new cities in China. *Sci. Geogr. Sin.* **1998**, *18*, 320–327.
80. Guldin, G.E. Urbanizing China. In *The Development of Small Towns and their Role in the Modernization of China*; Ma, R., Ed.; Greenwood Press: New York, NY, USA, 1992; pp. 119–154.
81. Kanbur, R.; Zhang, X. Fifty years of regional inequality in China: A journey through central planning, reform, and openness. *Rev. Dev. Econ.* **2005**, *9*, 87–106. [CrossRef]
82. Lin, G.C.S. Development and planning of small towns in China: Speculation, reassessment and prospect. *Sci. Geogr. Sin.* **1997**, *13*, 24–30.
83. The Central People’s Government of the People’s Republic of China. The Fourth Session of the Sixth National People’s Congress. Available online: http://www.gov.cn/test/2006-02/24/content_209830.htm (accessed on 24 February 2006).
84. Wu, K.; Fang, C.L. The development process and basic pattern of China’s small towns since 1949 and its recent new situation. *Econ. Geogr.* **2009**, *29*, 1605–1611.
85. Qian, Z. Land acquisition compensation in post-reform China: Evolution, structure and challenges in Hangzhou. *Land Use Policy* **2015**, *46*, 250–257. [CrossRef]
86. State Council of China. The National New Type Urbanization Plan (2014–2020). Available online: <http://www.gov.cn/zhuanti/xxczh/index.htm> (accessed on 16 March 2014).
87. Liu, N.; Liu, C.; Xia, Y.; Da, B. Examining the coordination between urbanization and eco-environment using coupling and spatial analyses: A case study in China. *Ecol. Indic.* **2018**, *93*, 1163–1175. [CrossRef]
88. Wei, Y.; Zhao, M. Urban spill over vs. local urban sprawl: Entangling land-use regulations in the urban growth of China’s megacities. *Land Use Policy* **2009**, *26*, 1031–1045.
89. Sui, D.Z.; Zeng, H. Modeling the dynamics of landscape structure in Asia’s emerging desakota regions: A case study in Shenzhen. *Landsc. Urban Plan.* **2001**, *53*, 37–52. [CrossRef]

